Utilisation of underwater acoustic backscatter systems to characterise nuclear waste suspensions remotely

Serish Tanya Hussain, Timothy N. Hunter, Jeffrey Peakall, and Martyn Barnes

Citation: Proc. Mtgs. Acoust. **40**, 070005 (2020); doi: 10.1121/2.0001303
View online: https://doi.org/10.1121/2.0001303
View Table of Contents: https://asa.scitation.org/toc/pma/40/1
Published by the Acoustical Society of America

Volume 40 http://acousticalsociety.org/

International Conference on Underwater Acoustics

9 September 2020

ICUA 2020

Utilisation of underwater acoustic backscatter systems to characterise nuclear waste suspensions remotely

Serish Tanya Hussain and Timothy N. Hunter
School of Chemical and Process Engineering, University of Leeds, Leeds, West Yorkshire, LS2 9JT, UNITED KINGDOM; pm14sth@leeds.ac.uk; t.n.hunter@leeds.ac.uk

Jeffrey Peakall
School of Earth and Environment, University of Leeds, Leeds,West Yorkshire, LS2 9JT, UNITED KINGDOM; j.peakall@leeds.ac.uk

Martyn Barnes
Sellafield Ltd, Warrington, Cheshire, WA3 6GR, UNITED KINGDOM; martyn.g.barnes@sellafieldsites.com

This paper reports application of ABS (Acoustic Backscatter Systems) to address nuclear waste management within the UK. ABS offers a route towards an online monitoring system to characterise wastes safely and remotely in real-time, during pipeline transportation; resulting in reduced hazard reduction timescales and taxpayer cost savings. Here, an ultrasonic velocimetry profiler (UVP) was used to analyse glass dispersions of varying concentrations, to assess online waste monitoring applicability. Acoustic backscatter profiles were collected to establish attenuation coefficients for two glass sizes (~40 and 80 μm) with 2 and 4 MHz probes. The 4 MHz probes were the most highly attenuating while transducer active radius had a negligible effect on probe sensitivity with either glass. A calibration procedure was used to measure sediment attenuation coefficients, which were compared to model estimates and experimental literature. For most systems, measured coefficients were close to estimated values, highlighting improved calibration accuracy, due to the mixing tank used. However, values for the smaller glass and 2 MHz probes overestimated model predictions, due to additional viscous attenuation. The measured value for the larger glass with 4 MHz probes was underestimated, this was caused by high attenuation reaching the instrument noise-floor, limiting the region available for analysis.

Published by the Acoustical Society of America

 https://doi.org/10.1121/2.0001303

1. INTRODUCTION

The change from military to civil use of nuclear energy in the UK was pioneered using the first fleet of Magnox reactors. All spent fuel from Magnox reactors was sent to Sellafield[1], where the magnesium alloy fuel cladding was kept long-term in a number of storage ponds. Over time, conditions have led to corrosion of the magnesium to a precipitated magnesium hydroxide-based sludge[2,3], which have complex particulate properties, while aggregates may undergo further changes from shear degradation during transportation[4]. Additionally, long term changes to pond chemistry and ingress of additional contamination have altered the composition of these wastes[5], making characterisation complex and problematic. Sellafield are currently transporting these sludges through engineered pipelines to treatment and containment facilities, where remote, online or *in situ* characterisation techniques could provide knowledge of the physical properties of the sludge (e.g. size and concentration) expediting its safe and economic treatment[4,6]. From previous literature and knowledge of acoustics, the priority systems to be investigated are acoustic backscatter systems (ABS)[7,8,9,10]. These systems have been used extensively in marine or estuarine environments and generally use single frequency transducers that act as combined transmitter-receivers[11,12]. ABS have been used to profile sediment concentration, by measuring the attenuation from the echo response of signal penetrated through the water. More recently, similar systems have been used to characterise industrial suspensions (e.g. *in situ* within mixing tanks or during transportation from pipe walls) making it a potentially important online technique for process monitoring and control[13,14]. The suspension attenuation rate depends on several system properties, such as particle size distribution, probe frequency and concentration. By analysing the received transducer strength and generating backscatter profiles as a function of distance, correlations between concentration differences or variations in material properties can be established[11].

Several types of ABS have been used for studies of waste dispersions, such as the AQUA scat 1000[10,15], UVP-DUO[13,16,17] and the UARP[4,18,19]. The UARP is a bespoke precommercial system produced by the University of Leeds, which has some restrictions on the ability to modify instrumental parameters, potentially limiting widescale industrial adoption. Therefore, for this project, an existing commercial system was deemed more beneficial[18], where data can be easily reproduced, and parameters transferred to any researcher within the field[13]. The AQUA scat 1000 has a range of seven frequencies from 300 kHz to 5 MHz, with the transducers having an active radius from 10–25 mm[20]. However, a 10–15 mm radius range would likely be too large for use on most nuclear waste pipeline applications, as the average pipe diameter is normally in the order of 50 mm[21]. The UVP-DUO has a frequency range from 1–8 MHz, which is large enough to analyse most relevant dispersions, while the active radii for the transducers are a smaller 2.5–10 mm, where 2.5 or 5 mm is ideal for non-intrusive attachment on pipelines[13]. Therefore, for this project, a commercial UVP-DUO was assessed for its ability to characterise relevant suspensions.

Rice *et al.*[13,21] previously conducted acoustic backscatter measurements with a UVP-DUO (which is normally utilised as a Doppler velocity profiler) to characterise glass and plastic slurries, for pipeline applications. Their work also included the development of a simple method to measure the sediment attenuation coefficients, which were used to establish concentration profiles. Unfortunately, the lack of a consistent calibration mixing unit limited the level of data correlation to verify the accuracy of the UVP-DUO. Indeed, before extracting echo profiles, any measurement system must be calibrated to optimise results, where materials with known acoustic properties in suspension are used to correct the instrumental setup[22]. Bux *et al.*[23] furthered the work of Rice *et al.*[9], in developing a robust, straightforward technique for the analysis of acoustic dispersion calibration data, which will be utilised in the present study.

A series of sediment specific parameters can be calculated from acoustic profiles; including the sedimentation attenuation coefficient, backscattering coefficient, normalised scattering cross section and scattering form function. The latter two dimensionless numbers correlate the overall scattering and attenuation properties of the dispersions and can be estimated for spherical particles from heuristic models, as found in Betteridge *et al.*[24] and Thorne and Hanes[22]. Betteridge *et al.*[24] derived expressions specifically for spherical glass particles whilst Thorne and Hanes[22] were derived for quartz-type sand particles. Several researchers have also theoretically considered the influence of particle size or concentration on the acoustic backscatter response, such as Moore *et al.*[25], who predicted the relationship between attenuation and particle radius between different materials. Butler and Sherman[26] stated that for high concentration

dispersions, sound will propagate at a higher rate through non-directional scattering, as the signal is reflected between the large magnitude of particles, while at lower concentrations, the signal is more likely to be reflected back to the transducer. For particles < 100 μm, which is the expected size region of nuclear waste sludges, higher frequency probes are preferred as they are more sensitive to differences in concentration.

Given this establishing literature, there is significant potential for ABS to be utilised as pipe flow slurry monitors. However, there are still several questions remaining into the performance of current commercial profilers to characterise systems of relevance to the nuclear industry. Therefore, this study aims to improve acoustic calibration procedures and determine accurate backscatter profiles of fine (< 100 μm) particles, using a commercial UVP-DUO. Two sizes of spherical glass dispersions are analysed, as their scattering-attenuation properties can be correlated to known theoretical models. Whilst the methodology outlined by Rice *et al*.[9,13] has previously been used to produce attenuation coefficients with similar instruments, coefficient values were up to an order of magnitude off estimations from heuristic expressions by Betteridge *et al*.[24]. Thus, a major objective of this work is to improve the calibration procedure, to better demonstrate the accuracy of this commercial device for backscatter applications. A modified recirculation mixing tank is utilised for this purpose, allowing the characterisation of the particle dispersions with various transducer sizes and frequencies. The project itself will ultimately build on this research to produce a fully remote online characterisation tool for pipeline waste slurries, which has not been achieved with high accuracy.

2. ACOUSTIC THEORY

The general acoustic model utilised is summarised from Thorne and Hanes[22] and shown in Eq. (1). Here, the backscatter voltage (V_{rms} in V) is written in terms of the distance from the transducer (r, in m), particle concentration (M, in kg.m^{-3}), nearfield correction factor (ψ, which is unity in the farfield, as assumed in this study) and the transducer constant (k_t in V.m$^{1.5}$) which approximates the electro-mechanical material losses in the transducer. It is also a function of two critical particle material factors, the backscatter coefficient (k_s, in m.kg$^{-0.5}$) and overall attenuation coefficient (α, in m^{-1}).

$$V_{rms} = \frac{k_s k_t}{\psi r} M^{\frac{1}{2}} e^{2r\alpha} \tag{1}$$

The overall attenuation coefficient, $\alpha = \alpha_s + \alpha_w$, where α_w is the attenuation due to water (and can be estimated from literature correlations[21, 27]) while α_s is the particle attenuation due to scattering losses. The particle attenuation is normally given in terms of the concentration independent sedimentation attenuation coefficient (ξ, in m^2.kg^{-1}) and particle concentration (M, in kg.m^{-3}), as shown in in Eq. (2).

$$\alpha_s = \xi M \tag{2}$$

The sedimentation attenuation coefficient, can be estimated from Eq. (3), as a function of the normalised scattering cross-section (χ, dimensionless) as well as the particle density (ρ, in kg.m^{-3}) and particle radius (a, in m)[22].

$$\xi = \frac{3\chi}{4\rho a} \tag{3}$$

The backscattering constant (k_s, in m.kg$^{-0.5}$) is calculated from Eq. (4), as a function of the form function (f, dimensionless) and particle density and radius[22].

$$k_s = \frac{f}{\sqrt{\rho a}} \tag{4}$$

The normalised scattering cross-section and the form functions can be estimated using heuristic expressions from Thorne and Hanes[22] and Betteridge *et al*.[24]. Thorne and Hanes[22] developed expressions for quartz particles, while Betteridge *et al*.[24] established models for spherical glass particles. The expression for the normalised scattering cross-section from Betteridge *et al*.[24], is shown in Eq. (5) and will be used to correlate measured data. It is a function of the angular wavenumber (k, in m^{-1}) and particle radius (a, in m).

$$\chi = \frac{0.24\left(1-0.4e^{-\left(\frac{ka-5.5}{2.5^2}\right)}\right)(ka)^4}{0.7+0.3(ka)+2.1(ka)^2-0.7(ka)^3+0.3(ka)^4} \quad (5)$$

Alternatively, the attenuation coefficient can be directly measured for any arbitrary dispersion, using an approach detailed by Rice *et al.*[21] and Bux *et al.*[8], from a logarithmic linearisation of Eq. (1), as given in Eq. (6), entitled the *G*-function. The range corrected natural log of the echo amplitude (*G*, in ln(Vm)) is given as a function of distance away from the transducer (*r*, in m), voltage (*V*, in Volts) and the near field correction factor (ψ, which is assumed to be unity)[21].

$$G = ln(\psi rV) = ln(k_s k_t) + \frac{1}{2} lnM - 2r(\alpha_w + \alpha_s) \quad (6)$$

The attenuation can be directly gained from taking a double differential of the *G*-function, as given in Eq. (7).

$$\xi = -\frac{1}{2}\frac{\partial^2 G}{\partial M \partial r} = -\frac{1}{2}\frac{\partial}{\partial M}\left[\frac{\partial}{\partial r}[\ln(\psi rV)\right] \quad (7)$$

Practically, in calibration procedures, the average linear gradient of *G* versus distance (d*G*/d*r*) can be measured for different particle systems at specific concentrations, where the attenuation coefficient can then be calculated directly from the average gradient change in these values versus concentration (*M*).

Finally, Eq. (8) is used specifically for the UVP-DUO to convert raw measured echo amplitude data (*E(r)*) into voltage (*V(r)*). The calculated voltage is also dependent on the instrument gain function (*g(r)*). The gain function is user identified, ranging from 1–9[21].

$$V(r) = \frac{3.052\times10^{-4}E(r)}{g(r)} \quad (8)$$

3. MATERIALS & METHODOLOGY

A. MATERIALS

Two sizes of glass dispersions were used as the calibration material to extract attenuation coefficients: Honite-22 and Honite-16 (Guyson Ltd[28]). For ease of understanding these are called ‘small’ and ‘large’ glass, respectively. Their average particle size distributions (PSDs) are given in Fig. 1, as measured by laser diffraction using a Mastersizer 2000 (Malvern Panalytical Ltd). The two materials should acoustically have discernibly different scattering attenuation profiles, based on Moore *et al.*[25], while they are spherical particles that can be heuristically modelled (as given in Eq. (5))

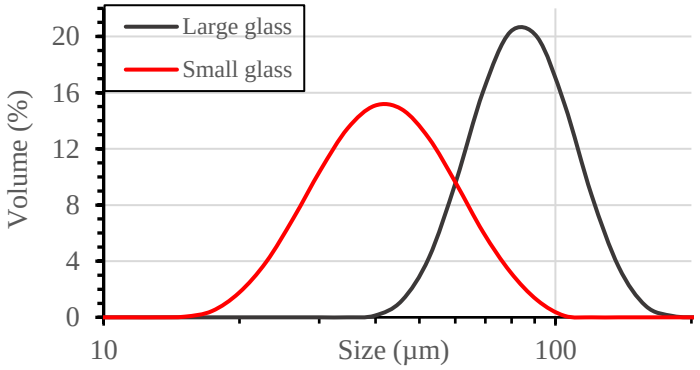

Figure 1. Particle size distributions for two Soda-lime glass dispersions.

B. ACOUSTIC CALIBRATION

All experiments were conducted with a commercial ultrasonic velocity profiler (UVP), using a UVP-DUO (MetFlow S.A.) where the backscatter amplitude signal was extracted as outlined in Eq. (8). To understand any

variation with system parameters, two 2 MHz probes with 2.5 mm and 5 mm active radii were used, along with a 4 MHz probe with a 2.5 mm active radius. A summary of the experimental UVP testing parameters is given in Table 1, where it is noted importantly, the backscatter was profiled to a maximum distance of ~30 cm for each measurement.

Table 1. UVP-DUO testing parameters.

Number of bins	272
Number of profiles	1024
Sampling period	42 ms
Speed of sound	1,480 m/s
Maximum depth	398.86 mm
Pulse repetition frequency	1/86 kHz
Minimum-maximum measurement distance (mm)	0.37 mm – 301.18 mm
Channel distance	1.11 mm
Channel width	3.7 mm
Angle	90º
Frequency of transducer	2, 4 MHz
Repetitions	48
Noise level	4
US Voltage	150 V
Gain start and end	6 - 6

All experiments were conducted in a baffled, recirculating calibration tank with a conical base, which was designed to generate well mixed suspensions that are completely invariant in particle concentration or size with depth. A schematic of the set-up is shown in Fig. 2. The particle concentration range tested was from 11.9–107.5 g/l for the two sets of glass dispersions. The tank was also tested using just water as a control, and glass powder was added for each concentration underneath the waterline to prevent air entrainment. The system was left for 2 minutes to fully disperse and the suspension was analysed with the transducers consecutively. All transducers were tested within the same suspension and data was collected consecutively from each, ensuring the set-up for each transducer was identical. The transducers were mounted fully submerged within the tank, in the upper quadrant, to avoid reflections from the impeller mixer. The probes were replaced with one after another for each concentration, but were mounted in the same place. The mixer was maintained at 150 rpm, with the recirculation pump at 130 rpm.

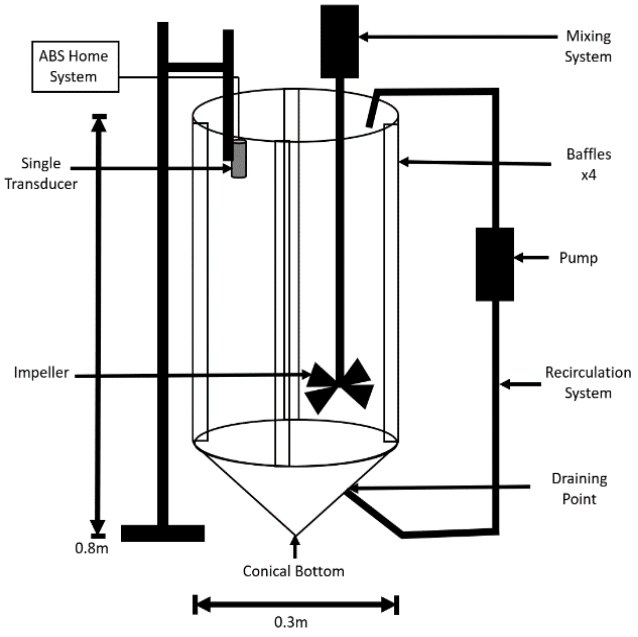

Figure 2. Schematic of recirculating calibration tank.

4. RESULTS AND DISCUSSION

A. LARGE GLASS

Figures 3 & 4 present the acoustic responses for the large glass dispersions, corresponding to the two different 2 MHz transducers (2.5 mm and 5 mm active radii) respectively. Each figure shows two profiles; (a) the decibel backscatter profile from the transducer and (b) the range corrected *G*-function profile ($G = ln(Vr\psi)$). A few general observations can be noted. Importantly, greater particle concentrations correlate to steeper gradients in the backscatter signal and *G* (at least within the farfield, for distances > 0.1 m), representative of greater signal attenuation due to elevated levels of particle scattering. A peak is also detected at 0.3 m, which is produced by an impeller reflection, highlighting that the backscatter profile is detecting all obstructions. A range from 0.1 – 0.2 m was taken to measure the linear gradient (d*G*/d*r*) in (b), to estimate the attenuation coefficient, for both transducer systems. It is observed that the values of *G* for distances < 0.1 increase significantly with distance before inflecting because of nearfield interferences, and thus are ignored. It would also be expected that the nearfield region would be greater for the larger 5 mm radius transducer, which is consistent with the presented data (noting the points of inflection in the *G*-function for each concentration are at greater distances for the 5 mm radius probe).

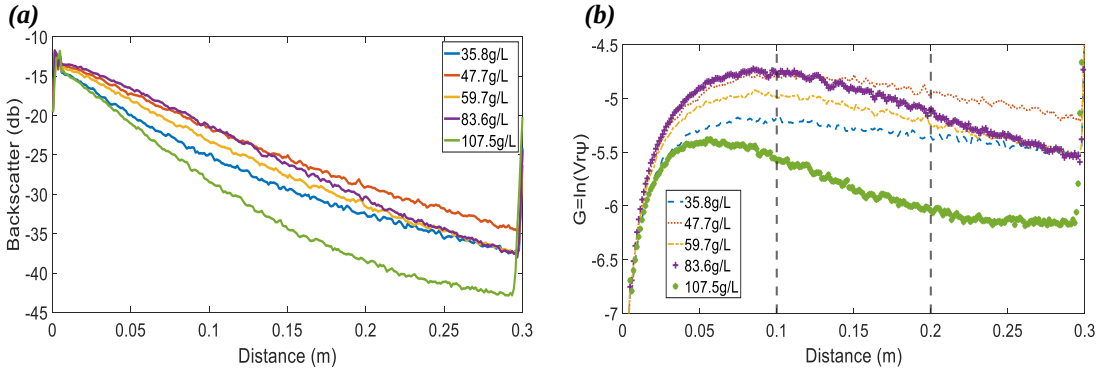

Figure 3. (a) Acoustic backscatter and (b) G-function vs distance for large glass dispersions at various concentrations using a 2 MHz probe with a 2.5 mm active radius. Dashed vertical lines in indicate linear region.

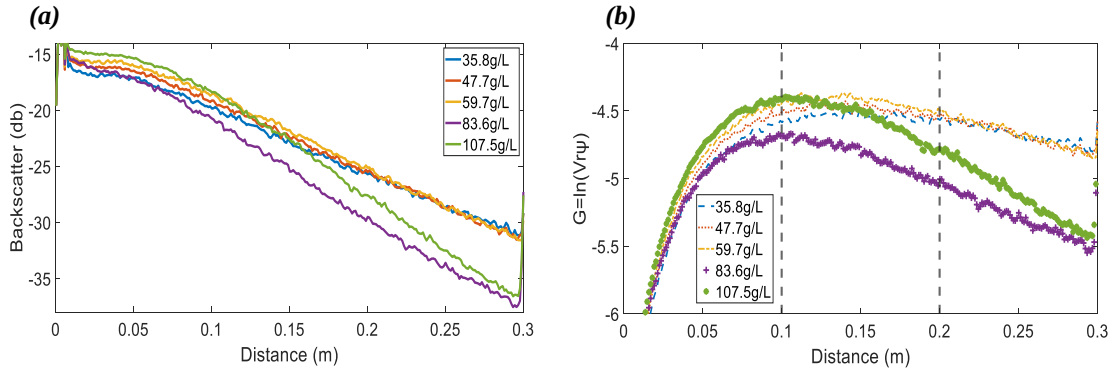

Figure 4. (a) Acoustic backscatter and (b) G-function vs distance for large glass dispersions at various concentrations using a 2 MHz probe with a 5 mm active radius. Dashed vertical lines in indicate linear region.

Figure 5 (a) and (b) shows backscatter and *G*-function distance profiles respectively for the large glass, using the 4 MHz transducer with 2.5 mm active radius. It is evident from Fig. 5 that the acoustic signal attenuates to a much greater degree with the 4 MHz probes for a given concentration than for the 2 MHz transducers, which would be expected given the smaller wavelength of the pulse. Indeed, the high attenuation led to the signal hitting the instrument noise-floor at intermediate distances, which results in the apparent second inflection point in the *G*-function profile with distance (and is simply an artefact from the weak signal). Therefore, a smaller distance range of 0.05–1 m was chosen to take the linear gradients (d*G*/d*r*) at each concentration for calculation of the attenuation coefficient. It is noted the nearfield interference region is also reduced for this small probe size and high frequency[29].

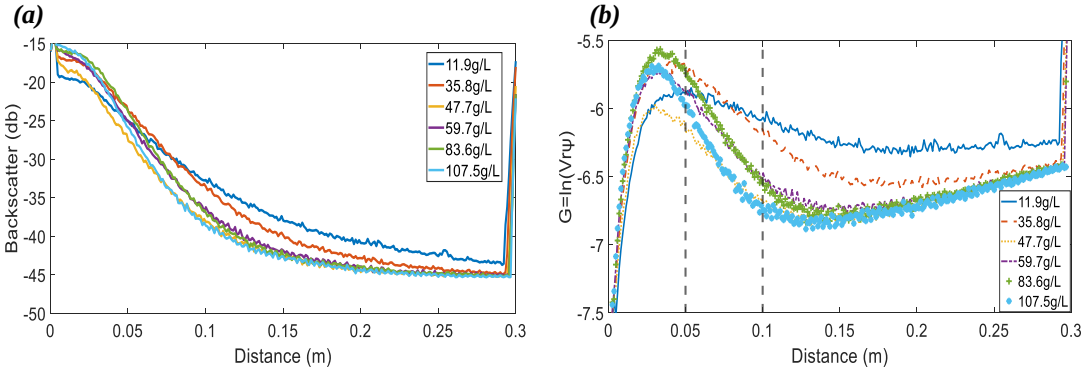

Figure 5. (a) Acoustic backscatter and (b) G-function vs distance for large glass dispersions at various concentrations using a 4 MHz probe with a 2.5 mm active radius. Dashed vertical lines in indicate linear region.

B. SMALL GLASS

Figures 6 & 7 present corresponding acoustic profiles for the small glass dispersions, with the 2 MHz 2.5 mm and 5 mm active radii respectively, again showing the backscatter strength in (a) and *G*-function in (b).

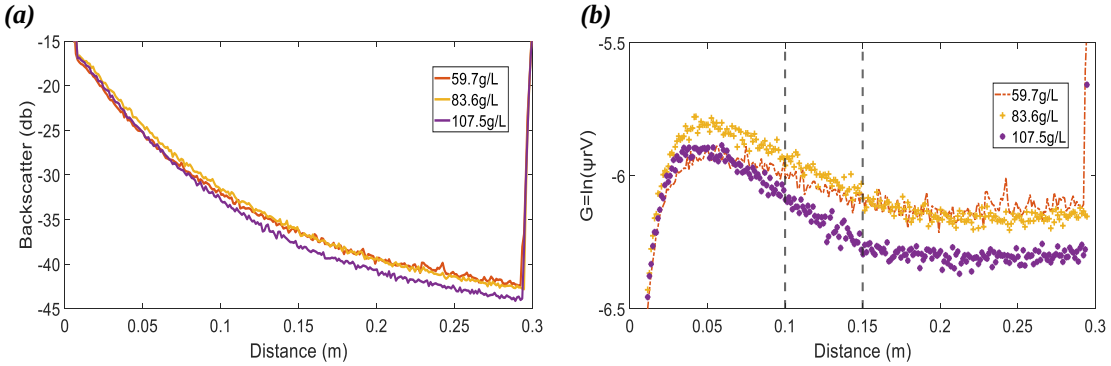

Figure 6. (a) Acoustic backscatter and (b) G-function vs distance for small glass dispersions at various concentrations using a 2 MHz probe with a 2.5 mm active radius. Dashed vertical lines in indicate linear region.

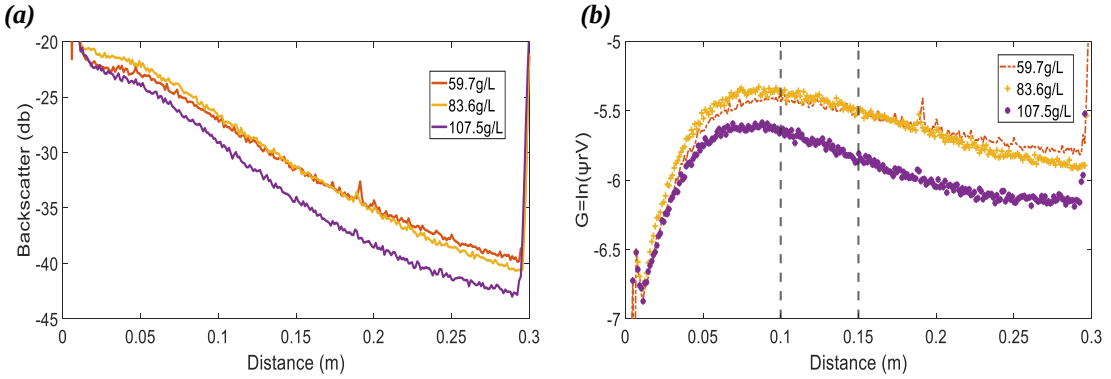

Figure 7. (a) Acoustic backscatter and (b) G-function vs distance for small glass dispersions at various concentrations using a 2 MHz probe with a 5 mm active radius. Dashed vertical lines in indicate linear region.

As considered by Moore *et al.*[25], the smaller glass would be expected to scatter a significantly lower proportion of the sound waves. This reduction presents itself as differences to both the backscattering strength and signal attenuation. When comparing the backscatter strength data between the glass sizes for the smaller transducer (e.g. Fig. 6 (a) to Fig. 3 (a)) the distance average signal strength remains > -40 dB for all particle levels with the larger glass, apart from the very highest concentration tested. Conversely, the backscatter signal for all concentrations with the

smaller glass decreases to approximately -45 dB at intermediate distances (correlating to the probe noise-floor). Similar characteristics are evident when the large transducer backscatter data is compared between the particle sizes (noting, in general, the larger transducer leads to higher average signal strengths in both cases, giving additional signal range).

The differences in signal attenuation as concentration increases for the smaller glass are observed in changes to the *G*-function with concentration (Figs. 6 & 7 (b)). The gradients in the *G*-function (d*G*/d*r*) for each corresponding particle concentration are slightly reduced with the smaller glass in comparison to the larger particles (when taken from the given linear regions) as expected for lower attenuating species[23,25]. However, some further complications arise. Firstly, it is evident with the smaller transducer (Fig. 6 (b)) that the low average backscatter level with the small glass leads to the signal becoming very weak and approaching the noise-floor at intermediate distances (leading to a second inflection of the G-function versus distance, as observed for the 4 MHz large glass particles in Fig. 5). Therefore, a smaller region was taken to quantify the linear gradients (0.1 to 0.15, as indicated). Additionally, it would be expected that particles of a mean size of ~40 µm may also attenuate sound via viscous absorption mechanisms, in addition to scattering[23], which would elevate the level of overall attenuation, reducing the measured differences to the large glass.

Figure 8 (a) and (b) show the backscatter and *G*-function profiles respectively for the small glass using a 4 MHz probe. As with the large glass (Fig. 5 (b)) an apparent second inflection in the *G*-function versus distance profile is observed, at ~0.15 m for all concentrations, which is an artefact of a weak signal approaching the transducer noise-floor. Thus, again, a closer linear region was taken from 0.05–0.1 m to estimate d*G*/d*r* values. Nonetheless, it is evident that the smaller glass leads to significantly lower levels of attenuation for the 4 MHz frequency probe (observed from the lower average d*G*/d*r* gradient values for particular concentrations) in comparison to the 2 MHz data. This result is consistent with theories of scattering and viscous losses, where higher frequencies lead to scattering dominant interactions.

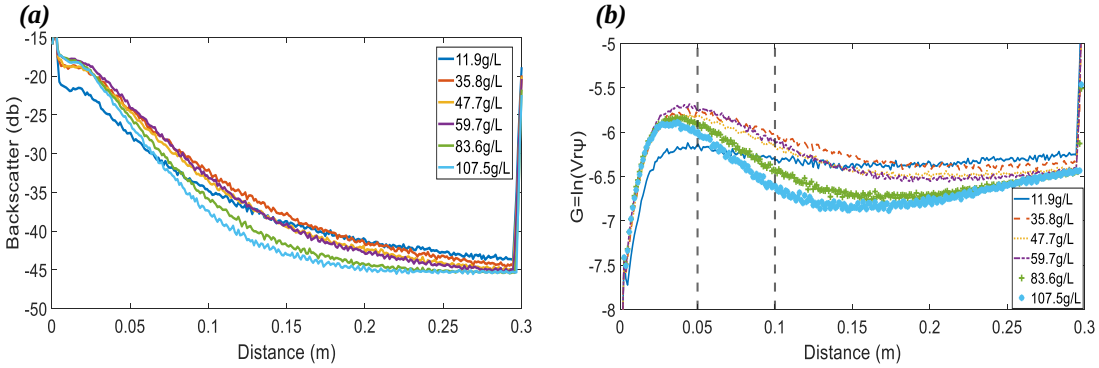

Figure 8. (a) Acoustic backscatter and (b) G-function vs distance for small glass dispersions at various concentrations using a 4 MHz probe with a 2.5 mm active radius. Dashed vertical lines in indicate linear region.

C. MEASURED ATTENUATION COEFFICIENTS AND MODEL ESTIMATES

The quantified average linear gradients of the *G*-function profiles for all systems (d*G*/d*r*, in Neper per metre) was compared, in terms of the particle concentration (*M*), as shown Figure 9 (a). Here, the average gradient change versus concentration for each transducer-particle pairing was estimated (shown by the dashed lines in the figure) and used to calculate the independent attenuation coefficient, ξ (as given by Eq. (7)). Additionally, the dimensionless scattering cross-section (χ) could then be calculated for each system (through rearrangement of Eq. (3), where particle density was taken as 2500 kg.m^{-3}, as for glass). The measured χ values for all systems studied are compared to the Betteridge *et al.*[24] heuristic model estimation (calculated from Eq. (5) by varying *ka*) in Fig. 9 (b). Additionally, the measured attenuation coefficients are compared to calculated estimates, also from the Betteridge model, as well as experimentally determined values for the same sized particle systems measured previously by Bux *et al.*[23] using a different type of ABS (AquaScat1000), shown in Fig. 9 (c).

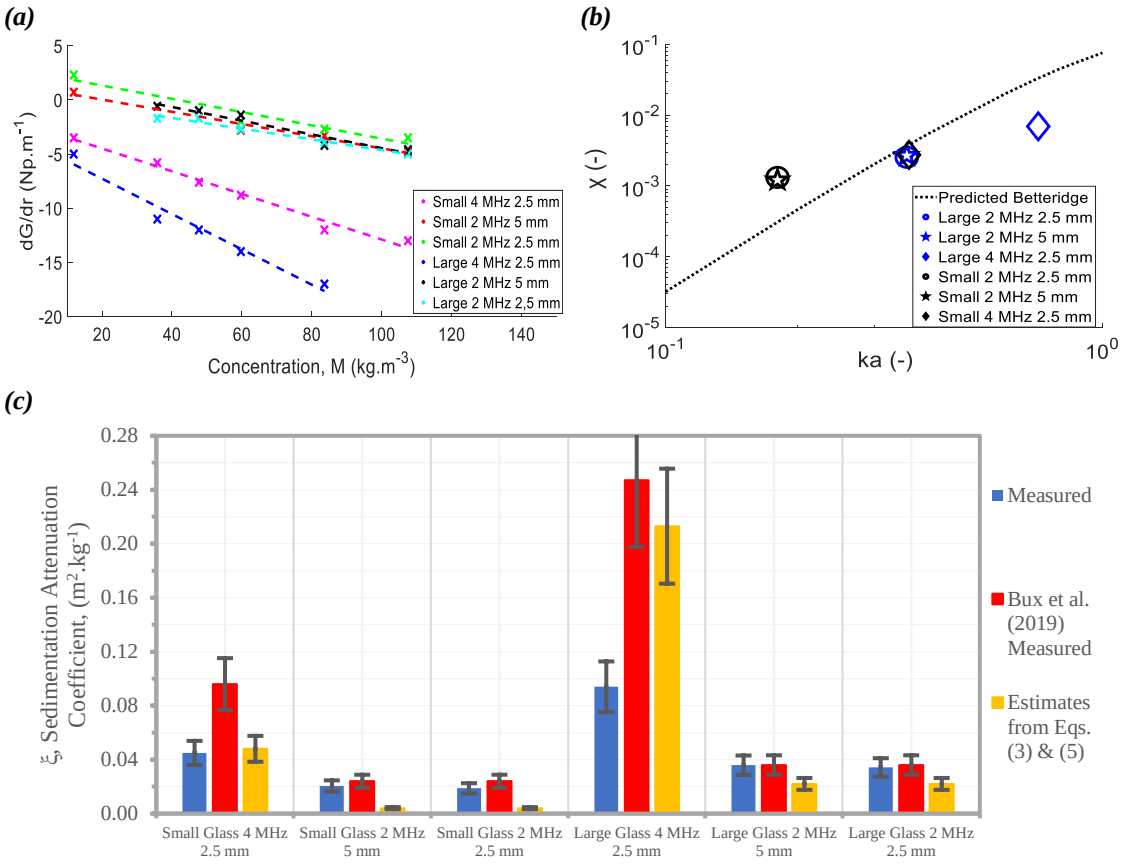

Figure 9. (a) Change in dG/dr vs concentration for both particle sizes and all transducers. (b) Dimensionless scattering cross-section (χ) vs product of the wavenumber and particle radius (ka) for all experimental systems in comparison to the scattering model of Betteridge et al.[24]. (c) Measured concentration independent, sediment attenuation coefficients for all systems, in comparison to model estimations from Betteridge et al.[24] (using Eqs. (3) and (5)) as well as previous measurements from Bux et al.[23].

As shown in Fig. 9 (b), the normalised scattering cross section (χ) values increase with frequency and particle size, as would be expected[24,22]. The values for the large glass, measured with both 2 MHz probes, as well as the small glass value measured with the 4 MHz probe, compare very closely to spherical particle predictions of Betteridge *et al.*[24]. It is noted that as the large glass is approximately double the mean size of the small glass, while the 4 MHz probe has a wavelength that is one half of the 2 MHz probe, these systems have almost identical *ka* terms. It is also emphasised that as estimations of the large and small transducers for each glass overlay precisely, it indicates both transducers are performing as predicted for calibration (as there should be no dependence of transducer properties on measured attenuation coefficients for a given frequency). Indeed, in general, the χ estimations are closer to predictions than previous measurements from Rice *et al.*[9], highlighting the designed recirculation calibration tank gives superior particle dispersion. However, there are clearly certain systems that compare less well to the estimated values. In particular, the small glass values, measured by both 2 MHz probes, give values that are considerably greater than predicted. It is assumed this is because of enhanced viscous absorption attenuation with small particles and the lower 2 MHz frequency transducers, where the given prediction is only based on scattering attenuation. Similar measured enhancements have been observed for particles in the same size range by Bux *et al.*[23]. Additionally, the 4 MHz coefficient for the larger glass is underestimated. It is assumed that this is due to high scattering attenuation losses for this probe. As outlined previously, this led to the signal decaying rapidly towards the noise-floor of the instrument at intermediate distances, significantly limiting the linear attenuation range. This problem could be overcome, in future work, by utilising a lower particle concentration range for 4 MHz calibration and incorporating a nearfield correction factor, improving the accuracy of the measurements closer to the region of the transducer[26].

Figure 9 (c) shows all sedimentation attenuation coefficients calculated for the six experiments. Coefficients measured from Bux *et al*.[23] (for identically sized glass dispersions) and estimated from the Betteridge *et al*.[24] model are displayed for validation. The error was calculated from the variation of echo amplitude across the measured distance (*r*), which was converted into maximum and minimum gradients. The maximum and minimum gradients were used to calculate the error range of sediment attenuation coefficients. All measured coefficient error bars overlap with coefficients produced in literature by Bux *et al*.[23] and Betteridge *et al*.[24]. The only coefficient, which is significantly different, is the value produced for the large glass 4 MHz test, which, as discussed, is likely due to high levels of scattering attenuation limiting the testing range.

5. CONCLUSIONS

In this study, two sizes of spherical glass dispersions (of ~40 and 80 μm) were characterised by acoustic backscatter, utilising a commercial ultrasonic velocity profiler (UVP). In particular, a well-mixed recirculating tank was used to determine the sediment attenuation coefficients, with two 2 MHz probes (of 2.5 mm and 5 mm active radii) and a 4 MHz probe (also of 2.5 mm active radius) following a calibration procedure outlined by Rice *et al*.[13]. Measured attenuation coefficients were compared to estimates produced by the Betteridge *et al*.[24] heuristic model for spherical particle scattering, as well as previous measurements on similar particle systems by Bux *et al*.[23]. Both sizes of 2 MHz probes produced consistent values of the attenuation coefficients, highlighting the smaller probe's applicability for online monitoring of pipeline slurries. However, the larger 2 MHz probe provided a higher accuracy of data due to the stronger backscatter return. Measurements using the 4 MHz probe were complicated owing to its high signal attenuation, leading to a very weak backscatter that approached the noise-floor of the instrument at intermediate distances for most concentrations. Nonetheless, using a small distance range, attenuation coefficients were still successfully determined. For most systems, attenuation coefficients correlated extremely well with model estimates and previous measured values, highlighting an improved calibration accuracy, due to the recirculating mixing tank used. However, results for the smaller glass with the 2 MHz probes show that theoretical predictions overestimate the actual values, due to additional viscous attenuation that is not captured in the models. Additionally, the measured value for the larger glass with the 4 MHz probe was underestimated in comparison to predictions, caused by the high attenuation limiting the region available for analysis. Future work will look at improving attenuation measurements with the 4 MHz probes, using lower particle concentrations. Additionally, a nearfield correction factor will be investigated and incorporated within the acoustic profiles, to improve signal accuracy for calibration at short distances, and for applications in online pipe flow monitoring, where geometries are constricted.

ACKNOWLEDGMENTS

The authors would like to acknowledge the Engineering and Physical Sciences Research Council (EPSRC) UK and Sellafield Ltd for funding through the Next Generation Nuclear (NGN) Centre for Doctoral Training (EP/L015390/1). Thanks, are also given to Geoff Randall from Sellafield Ltd for ongoing support.

REFERENCES

1. Barlow, S.T., Stennett, M.C., Hand, R.J., Morgan, S.P. and Hyatt, N.C. Thermal Treatment of UK Magnox Sludge. In: 2nd Petrus-OPERA PhD and early stage researcher conference proceedings. *OPERA Conference on Radioactive Waste Management and Geological Disposal proceedings, 27 June 2016, Delft.* Netherlands: Delft University of Technology, 2016, pp.19-22.

2. Gregson, C.R., Goddard, D.T., Sarsfield, M.J. and Taylor, R.J. Combined electron microscopy and vibrational spectroscopy study of corroded Magnox sludge from a legacy spent nuclear fuel storage pond. *Journal of Nuclear Materials.* 2011, **412**(1), pp. 145-156.

3. Johnson, M., Peakall, J., Fairweather, M., Barnes, M., Davison, S., Jia, X., Clare, M.A., Harbottle, D. and Hunter, T.N. Sediment Microstructure and the Establishment of Gas Migration Pathways during Bubble Growth. *Environmental Science and Technology.* 2019, **53**(21), pp. 12882-12892.

4. Hunter, T.N., Peakall, J., Egarr, D., Cowell, D.M.J., Freear, S., Tonge, A., Horton, L., Rice, H.P., Smith, I., Malone, K., Burt, D., Barnes, M., Randall, G., Biggs, S., Fairweather, M. Concentration profiling of a horizontal sedimentation tank utilising a bespoke acoustic backscatter array and CFD simulations. *Chemical Engineering Science.* 2020, **218**(1), pp. 1-12.

5. Burton, B. *Nuclear Power, Pollution and Politics.* London: Routledge, 2002.

6. Alderman, N.J. and Heywood, N.I. The Importance of Rheological Assessment in the Mobilisation, Mixing and Transport of Nuclear Waste Sludges. In: WM2011 Conference Proceedings. *Waste Management Conference 2011, 27 February 3 March 2011, Phoenix.* Phoenix: Waste Management Symposia, 2011.

7. Tonge, A., Usher, S. and Peakall, J. Use of In Situ Acoustic Backscatter Systems to Characterize Spent Nuclear Fuel and its Seperation in a Thickener. In: WM2019 Conference Proceedings. *Waste Management Conference 2019, 3-7 March 2019, Pheonix.* Phoenix: Waste Management Symposia, 2019.

8. Bux, J., Peakall, J., Biggs, S. and Hunter, T.N. In Situ characterisation of a concentrated colloidal titanium dioxide settling suspension and associated bed development: Application of an acoustic backscatter system. *Powder Technology.* 2015, **284**(1), pp. 530-540.

9. Rice, H.P., Fairweather, M., Hunter, T.N., Mahmoud, B., Biggs, S. and Peakall, J. Measuring particle concentration in multiphase pipe flow using acoustic backscatter: generalization of the dual-frequency inversion method. *Journal of the Acoustical Society of America.* 2014, **136**(1), pp. 156-169.

10. Hunter, T., Biggs, S., Young, J., Fairweather, M. and Peakall, J. Ultrasonic Techniques for the In Situ Characterisation of 'Legacy' Waste Sludges and Dispersions. In: ASME 2011 14th International Conference on Environmental Remediation and Radioactive Waste Management, Parts A and B. *International Conference on Radioactive Waste Management and Environmental Remediation, 17 August 2012, Reims.* Reims: ASME Digital Collection, 2012, pp. 801-806.

11. Gartner, J.W. Estimating suspended solids concentrations from backscatter intensity measured by acoustic doppler current profiler in San Francisco Bay, California. *Marine Geology*. 2004, **211**(1), pp. 169-187.

12. *Sa*hin, C., Verney, R., Sheremet, A. and Voulgaris, G. Acoustic backscatter by suspended cohesive sediments: Field observations, Seine Estuary, France. *Continental Shelf Research.* 2017, **134**(1), pp. 39-51.

13. Rice, H.P., Fairweather, M., Peakall, J., Hunter, T.N., Mahmoud, B. and Biggs, S. Measurement of particle concentration in horizontal, multiphase pipe flow using acoustic methods: Limiting concentration and the effect of attenuation. *Chemical Engineering Science.* 2015, **126**(1), pp. 745-758.

14. Rice, H.P., Peakall, J., Fairweather, M. and Hunter, T.N. Extending estimation of the critical deposition velocity in solid–liquid pipe flow to ideal and non-ideal particles at low and intermediate solid volume fractions. *Chemical Engineering Science.* 2020, **211**(1), pp. 1-9.

15. Bux, J., Paul, N., Hunter, T.N., Peakall, J., Dodds, J.M. and Biggs, S. In SItu Characterization of Mixing and Sedimentation Dynamics in an Impinging Jet Ballast Tank Via Acoustic Backscatter. *American Institute of Chemical Engineers.* 2017, **63**(7), pp. 1-12.

16. Kotze, R., Wiklund, J., Haldenwang, R. and Fester, V. Measurement and analysis of flow behaviour in complex geometries using the Ultrasonic Velocity Profiling (UVP) technique. *Flow Measurement and Instrumentation***.** 2011, **22**(2), pp. 110-119.

17. Birkhofer, B.H., Jeelani, S.A.K., Windhab, E.J., Ouriev, B., Lisner, K., Braun, P. and Zeng, Y. Monitoring of fat crystallization process using UVP-PD technique. *Flow Measurement and Instrumentation.* 2008, **19**(3), pp. 163-169.

18. Tonge, A.S., Bux, J., Hunter, T.N., Freear, S., Cowell, D.M.J. and Peakall, J. Concentration profiling using a novel acoustic backscatter system with single transducers pulsed at multiple frequencies. In: 2017 IEEE International Ultrasonics Symposium. *International Ultrasonics Symposium Proceedings, 6-9 September 2017, Washington*. Washington: IEEE, 2017.

19. Hunter, T.N., Cowell, D., Rice, H.P., Smith, I., Tonge, A., Freear, S., Randall, G., Barnes, M., Peakall, J., Malone, K., Burt, D., Horton, L., Egarr, D. and Biggs, S. Utilizing a Novel Acoustic Backscatter Array to Characterize

Waste Consolidation and Settling in a Horizontal Flow Clarifier. In: WM2016 Conference Proceedings. *Waste Management Conference 2016, 6-10 March 2016, Phoenix.* Phoenix: Waste Management Symposia, 2016.

20. Aquatec Group. *AQUAscat® 1000R*. [Online] 2020. [Accessed July 12, 2020]. Available from: http://www.aquatecgroup.com/aquascat/aquascat-1000r.
21. Rice, H.P. *Transport and deposition behaviour of model slurries in closed pipe flow.* Leeds: University of Leeds, 2013.
22. Thorne, P. and Hanes, M.D. A review of acoustic measurement of small-scale sediment processes. *Continental Shelf Research.* 2002, **22**(4), pp. 603-632.
23. Bux, J., Peakall, J., Rice, H.P., Manga, M.S., Biggs, S. and Hunter, T.N. Measurement and density normalisation of acoustic attenuation and backscattering constants of arbitrary suspensions within the Rayleigh scattering regime. *Applied Acoustics.* 2019, **146**(1), pp. 9-22.
24. Betteridge, K.F., Thorne, P.D. and Cooke, R. Calibrating multi-frequency acoustic backscatter systems for studying near-bed suspended sediment transport processes. *Continental Shelf Research.* 2008, **28**(2), pp. 227-235.
25. Moore, S.A., Le-Coz, J., Hurther, D. and Paquier, A. Using multi-frequency acoustic attenuation to monitor grain size and concentration of suspended sediment in rivers. *The Journal of the Acoustical Society of America.* 2013, **133**(4), pp. 1959-1970.
26. Butler, J.L. and Sherman, C.H. *Transducers and Arrays for Underwater Sound.* 2nd ed. London: Springer International Publishing, 2016.
27. Ainslie, M.A. and McColm, J.G. A simplified formula for viscous and chemical absorption in sea water. *Journal of the Acoustical Society of America.* 1998, **103**(3), pp. 1671-1672.
28. Guyson Ltd**.** *Glass Blast Media*. [Online]. 2020. [Accessed June 13, 2020]. Available from: https://s3-eu-west-1.amazonaws.com/resources.guyson.co.uk/product-downloads/Honite.pdf?mtime=20200117140801.
29. Kenneth, G. Discriminating between the nearfield and the farfield of acoustic transducers. *The Journal of the Acoustical Society of America.* 2014, **136**(4).